Strong Electron-Hole Exchange in Coherently Coupled Quantum Dots

Stefan Fält,[1] Mete Atatüre,[2] Hakan E. Türeci,[1] Yong Zhao,[3] Antonio Badolato,[1] and Atac Imamoglu[1]

[1]*Institute of Quantum Electronics, ETH Zurich, 8093 Zurich, Switzerland*

[2]*Cavendish Laboratory, University of Cambridge, Cambridge, CB3 0HE, United Kingdom*

[3]*Physikalisches Institut, Ruprecht-Karls-Universität Heidelberg, Philosophenweg 12, 69120 Heidelberg, Germany*

(Received 17 July 2007; revised manuscript received 13 January 2008; published 11 March 2008)

We have investigated few-body states in vertically stacked quantum dots. Because of a small interdot tunneling rate, the coupling in our system is in a previously unexplored regime where electron-hole exchange plays a prominent role. By tuning the gate bias, we are able to turn this coupling off and study a complementary regime where total electron spin is a good quantum number. The use of differential transmission allows us to obtain unambiguous signatures of the interplay between electron and hole-spin interactions. Small tunnel coupling also enables us to demonstrate all-optical charge sensing, where a conditional exciton energy shift in one dot identifies the charging state of the coupled partner.

DOI: 10.1103/PhysRevLett.100.106401 PACS numbers: 71.35.Cc, 71.70.Ej, 78.67.Hc

Self-assembled quantum dots (QDs) are semiconductor nanostructures that exhibit three-dimensional confinement of carriers. Because of spatial confinement, the electronic states in a QD are quantized, and these structures have been referred to as artificial atoms. This description has been verified experimentally with atomlike properties such as strong photon antibunching [1] and near lifetime limited linewidths [2]. One can use the self-assembly mechanism to create aligned nanostructures that function as QD molecules. Earlier studies have demonstrated hybridization of energy levels of two coupled QDs [3] and spectral signatures of tunnel coupling of multiple-hole [4,5] or two-electron [6] states. It has also been shown that the g-factor can be engineered by controlling the tunnel coupling [7]. Here, we use for the first time resonant differential transmission measurements to address each optical transition selectively in order to study the signatures of spin interactions in QD molecules with unprecedented spectral resolution. The interdot coupling in the QD molecules we studied is significantly modified by electron-hole exchange interaction. However, by changing the QD charging state via the gate voltage, we show that it is possible to turn electron-hole exchange completely off and investigate the regime dominated by electron-electron exchange coupling. In contrast to previous experiments, we were able to study optical emission and absorption from both QDs in the pair, which in turn allowed us to use interdot Coulomb interaction induced energy shifts to determine the charging state of both QDs.

The heterostructure we investigated was grown with molecular beam epitaxy on a GaAs substrate. The sample consists of a Schottky diode structure with two layers of InAs QDs in a GaAs matrix, both grown using the partially covered island technique [8]. The partial coverage was 1.3 nm for the first layer and 3.5 nm for the second, resulting in a larger blueshift for the first layer than the second. The QD layers will be referred to as the blue and red layers, respectively. The blue layer is separated from the n^+-GaAs back contact with 25 nm GaAs, and the red and blue layers are separated by 15 nm. The top gate consists of a semitransparent Ti layer. The red layer was spaced from the top gate with 160 nm GaAs, including an AlGaAs current blocking layer close to the top gate. A schematic band-edge diagram of the device can be seen in Figure 1(h). The strain field on top of QDs from the blue layer gives a natural alignment of the nucleation of QDs in the red layer so that stacks are formed.

The measurements were performed using microphotoluminescence (μ-PL) and differential transmission (DT) techniques at 4.2 K. For μ-PL, a 780 nm laser was used to create free carriers in the bulk GaAs. A lens with NA of 0.55 was used to both focus this laser and collect the luminescence, which was spectrally resolved with a resolution of 30 μeV. For DT measurements, a single frequency laser was tuned across the coupled QD resonances. A Si p-i-n photodiode detected the transmitted laser light, and a lock-in amplifier was used with DC stark-shift modulation of the resonances to eliminate low frequency noise [9].

The diode structure allows controlled electron charging of the QDs. As the stacking probability of the QDs is not unity, we were able to use single QDs without a coupled partner to investigate the spectral signatures of charging in the absence of inter-QD coupling. The gate-voltage-dependent PL spectra of these single QDs were qualitatively indistinguishable from previous reports on single-layer QDs [9]. The charging behavior of stacked QDs changes not only with the confining potential well depth, but also with the distance to the doped layer. In addition to emission wavelength, this difference in charging behavior between the layers aids us in the identification of which layer a certain QD is in.

The relatively large tunnel barrier between our dots allows us to study the emission properties of each QD of a pair with μ-PL. In Fig. 1, we present data from two pairs of coupled QDs (CQD1 and CQD2), focusing on three separate PL energy windows in the same gate voltage range. Figures 1(a) and 1(d) show the PL intensity lines of the negatively charged trion of the blue dot. Figures 1(b)

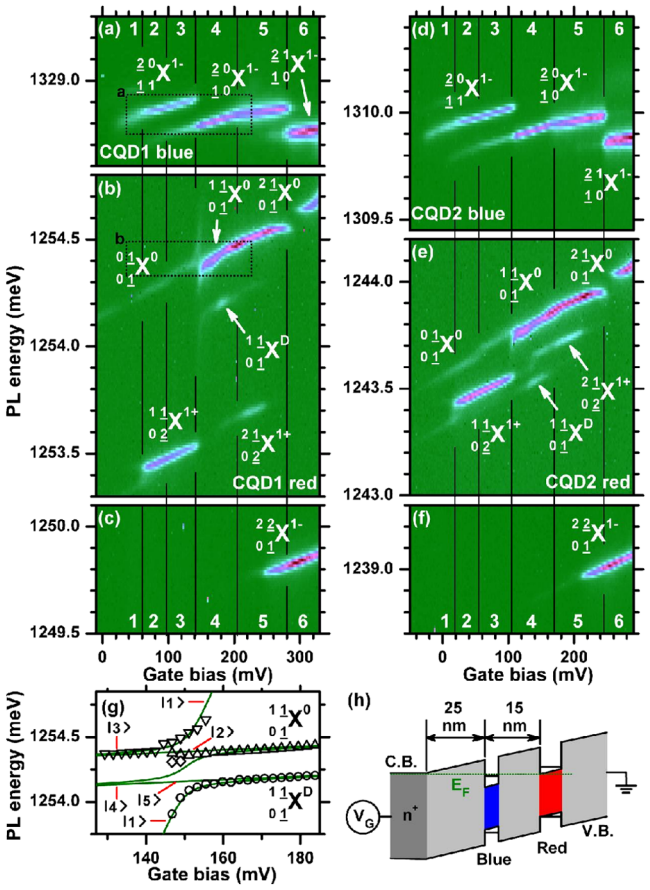

FIG. 1 (color online). PL plots of two different pairs of stacked QDs as a function of the applied gate bias where (a),(d) show PL data from the blue QDs of the pair, (b)–(c),(e)–(f) show the data from the red QDs. The PL lines are identified with the corresponding excitonic states, noted as $\alpha\beta\gamma\delta X^{\epsilon}$, where α (β) is the number of electrons in blue (red) QD, γ (δ) is the number of holes in blue (red) QD, ϵ is the type of exciton (with respect to the dot where recombining carriers reside), and underlines indicate which carriers pair-annihilate. Regions with different ground state charge combinations are separated with black vertical lines and numbered. Using the notation $\alpha\beta\gamma\delta G$, where G denotes the ground state these charge configurations are: 1: $^{00}_{00}G$ or $^{00}_{01}G$, 2: $^{00}_{00}G$ or $^{10}_{01}G$, 3: $^{10}_{00}G$ or $^{10}_{01}G$, 4: $^{10}_{00}G$, 5: $^{20}_{00}G$, and 6: $^{21}_{00}G$. The dotted rectangles indicate the regions where DT data (Fig. 2) was acquired. (g) Fitted PL data from (b) (scatter), specifically $^{11}_{01}X^{0}$ and $^{11}_{01}X^{D}$ and calculated optical transition energies as a function of gate bias (solid line) with the corresponding excited state marked. The calculation is based on a model that will be discussed later. (h) Schematic band-edge diagram of the device with the two dots labeled.

and 1(e) contain the lines for the neutral bright exciton (X^0), dark exciton (X^D), and positively charged trion (X^{1+}), while Figs. 1(c) and 1(f) show the negatively charged trion (X^{1-}) lines [10] for the red QDs. We first note that the X^{1-} line of the blue QDs in Figs. 1(a) and 1(d) is split into three, following closely the charging state of the corresponding red QD. In other words, the wavelength of the X^{1-} line of the blue QDs is conditional on the charging state of its stacked partner. The charge combinations for the excited state of the transitions are marked in Fig. 1, and the notation is explained in the figure caption [4]. The measured splittings between $^{21}_{10}X^{1-}$ and $^{20}_{10}X^{1-}$ (110 μeV) and $^{20}_{10}X^{1-}$ and $^{20}_{11}X^{1-}$ (130 μeV) are consistent with the expected dipolar shifts of the order of 100 μeV, estimated from the dc Stark shift of the lines. We note here that the shifts of the PL lines *in the red QD* due to charge sensing is in comparison smaller and in the opposite direction. The latter observation is easily explained by the charge inducing the energy shift being on the opposite side of the dipole as compared to the case of the blue QD. Small charge-sensing shifts of the red-QD PL lines may stem from strain-field induced modification of electron and hole wave functions and may be correlated to the X^{1+} line being redshifted as compared to the neutral exciton [11].

Signatures of coherent coupling in the X^0 line are apparent in the PL data of Fig. 1(b); remarkably, the assigned dark exciton line (X^D), 230 μeV on the red side of bright neutral exciton line also exhibits an anticrossing. Figure 1(g) shows a fit of the peak intensities of the PL data using a theoretical model we introduce below.

In order to investigate the spin fine structure in regions 3 and 4, we now focus on the DT measurements which provide higher resolution and eliminate spurious effects associated with the generation of free charges in the bulk GaAs. Figures 2(a) and 2(b) show data from the DT measurements carried out at zero external magnetic field on the blue and red QD, respectively. In these plots, the QDs are in the gate bias regime where we see X^{1-} absorption in the blue QD and X^0 absorption in the red QD. The blue QD shows a splitting in the DT signal due to the charge sensing that we noted earlier in the PL data. In contrast, the DT measurement on the red QD reveals several interesting features. For the gate voltage regime $V_G > 205$ mV, the X^0 line shows an unusually small anisotropic exchange splitting and a dc-Stark shift that increases with decreasing V_G. For $V_G = 205$ mV where one of the two excess electrons of the blue QD tunnels out into the back contact, the red QD DT absorption shows a kink. Further reduction of V_G leads to a splitting in the red QD absorption line that increases with decreasing V_G, signifying coherent coupling between the two QDs. Finally, for $V_G < 150$ mV, the DT signal completely disappears. Figure 2(c) shows the counterpart of Fig. 2(b) with an applied magnetic field of 0.4 T in the Faraday configuration [12]. Before discussing the coherent coupling regime of 150 mV $< V_G <$ 205 mV, we note that the disappearance of the DT signal for $V_G < 150$ mV is due to the fact that the optically generated electrons become unstable and tunnels out to the back contact. This observation is completely consistent with the appearance of X^{+1} PL line at precisely this gate voltage [Fig. 1(b)], since in this regime the red QD can be optically charged with an excess hole. The single DT line observed for $V_G > 205$ mV indicates

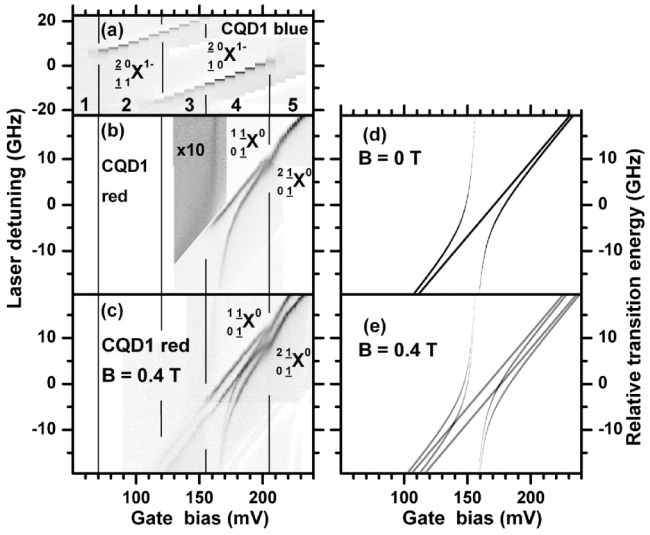

FIG. 2. (a) DT measurements showing two split lines for the blue X^{1-} due to charge sensing. Single hole charging of the red dot takes place by off resonant excitation with the DT laser and subsequent tunneling of the optically excited electron. (b) DT measurements on the red X^0 and (c) red X^0 in an external magnetic field of 0.4 T. (d) Calculated absorption without and (e) with magnetic field. In (b), we have magnified the weak absorption region in gray by $x10$.

that the anisotropic exchange splitting is smaller than the linewidth for this QD.

The results shown in Figs. 2(b) and 2(c) for 150 mV $< V_G <$ 205 mV indicate a different regime of coherent coupling from those realized in previous studies on CQDs [6], where electron-electron exchange was found to dominate the spin interactions. This can be seen most notably in the ratio of the transition strengths of the anticrossing and crossing branches which is about 1:1 [experiment, Fig. 2(b); theory, Fig. 2(d)] as opposed to the expected 1:3 with only indirect (interdot) electron exchange interaction. Based on a simple model that we present below, we attribute this qualitative difference to the tunnel coupling being relatively weak compared to the intradot electron-hole exchange interaction.

In anticipation of an electron-hole exchange interaction that is stronger than the tunnel-coupling, we use the following basis to describe the coherent coupling data

$$
\begin{aligned}
|1\rangle &= e^\dagger_{B\downarrow} e^\dagger_{B\uparrow} h^\dagger_{R\Uparrow}|0\rangle = (\downarrow\uparrow, \Uparrow), & |6\rangle &= (\downarrow\uparrow, \Downarrow),\\
|2\rangle &= e^\dagger_{B\downarrow} e^\dagger_{R\downarrow} h^\dagger_{R\Uparrow}|0\rangle = (\downarrow, B_+), & |7\rangle &= (\downarrow, B_-),\\
|3\rangle &= e^\dagger_{B\uparrow} e^\dagger_{R\downarrow} h^\dagger_{R\Uparrow}|0\rangle = (\uparrow, B_+), & |8\rangle &= (\uparrow, B_-),\\
|4\rangle &= e^\dagger_{B\downarrow} e^\dagger_{R\uparrow} h^\dagger_{R\Uparrow}|0\rangle = (\downarrow, D_+), & |9\rangle &= (\downarrow, D_-),\\
|5\rangle &= e^\dagger_{B\uparrow} e^\dagger_{R\uparrow} h^\dagger_{R\Uparrow}|0\rangle = (\uparrow, D_+), & |10\rangle &= (\uparrow, D_-).
\end{aligned}
$$

Here, $e^\dagger_{i\sigma}$ ($h^\dagger_{i\sigma}$) creates a spin-σ electron (hole) in the blue ($i = B$) or red ($i = R$) dot ($\Uparrow$, $\Downarrow$ refer to the hole pseudospin $J_z = \pm 3/2$). The states $|1\rangle$ and $|6\rangle$ form a spin singlet with both electrons in the blue QD and the other states are compositions of the one electron in the blue QD with a certain spin and a bright ($B_\pm$) or dark ($D_\pm$) exciton in the red QD, where "$\pm$" refers to excitation by right-hand or left-hand circular polarization. We assume that the hole due to energetic considerations is always in the red dot. The Hamiltonian has a block diagonal form due to vanishing anisotropic electron-hole exchange, which allows us to consider only the states from $|1\rangle$ to $|5\rangle$: For this system and basis states we have

$$
\begin{pmatrix}
d_i \frac{V}{l} + U & 0 & t_e & -t_e & 0\\
0 & E_1 & 0 & 0 & 0\\
t_e & 0 & E_1 & 0 & 0\\
-t_e & 0 & 0 & E_2 & 0\\
0 & 0 & 0 & 0 & E_2
\end{pmatrix},
$$

where $E_1 = \frac{1}{2}\delta_0 + d_d \frac{V_G}{l}$, $E_2 = -\frac{1}{2}\delta_0 + d_d \frac{V_G}{l}$, V_G is the applied gate bias, l is the distance between the back and top gates, d_i and d_d are the sizes of the effective indirect and direct static dipoles, and U is the intradot Coulomb interaction for two electrons in the blue QD measured with respect to their interdot Coulomb interaction. Further, t_e is the electron tunneling rate, and δ_0 is the isotropic electron-hole exchange interaction. We fit the DT data shown in Figs. 2(b) and 2(c) with t_e being the only adjustable fitting parameter [δ_0 and the Coulomb matrix elements are extracted independently from Fig. 1(b)]. The fitted DT absorption spectra yielding $t_e = 137$ μeV are displayed in Fig. 2(d) ($B = 0$) and 2(e) ($B = 0.4$ T). An important feature of this Hamiltonian is the coupling of the state $|1\rangle$ with the states $|3\rangle$ and $|4\rangle$ through the t_e term. The resulting hybridization of the dark and bright exciton states gives rise to a finite oscillator strength of the dark exciton $|4\rangle$ in a

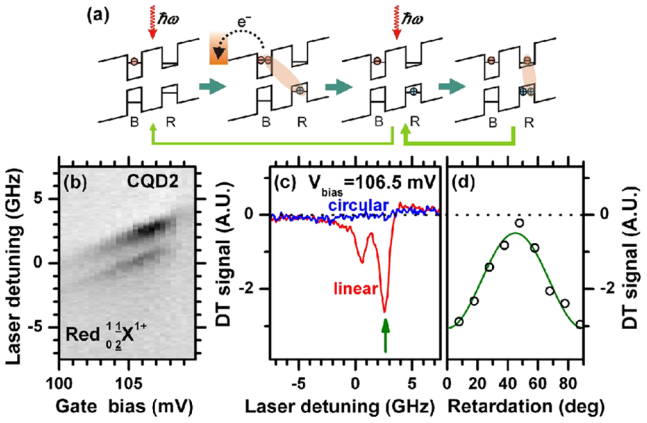

FIG. 3 (color online). (a) Schematic description of the two-photon process resulting in resonant excitation of the X^{1+} transition with only one resonant laser. (b) DT measurements of X^{1+} with excitation by only one laser. (c) Polarization dependence of the X^{1+} line, showing maximum absorption of linearly polarized light and minimal for circularly polarized light. (d) DT signal, with the resonant laser fixed at the strongest absorption peak [green arrow in (c)], as a function of the retardation (open circles) and a $\cos^2$ fit with an offset (solid line).

narrow gate bias regime around the anticrossing as seen in the PL data of Figs. 1(b) and 1(e) (line marked X^D). Another interesting feature of this Hamiltonian is that the electron-hole exchange interaction energetically splits the observed anticrossings for the parallel from the antiparallel spin of the electron with respect to the hole- spin.

We next investigate the gate bias regime which allows us to switch the electron-hole interaction off through an optical double-resonance. This process is described in Fig. 3(a) for CQD2 with PL data plotted in Fig. 1(e). For the red QD in the CQD2, the optically generated electron in the X^0 transition tunnels out at $V_G = 110$ mV. For a narrow gate voltage between 105–107 mV, the transition energy of the indirect X^0 and X^{1+} becomes equal due to the large dc-Stark shift of the indirect X^0. Since the final state of an indirect X^0 transition followed by a tunneling event into the back contact is the ground state of the X^{1+} transition, we can observe X^{1+} in DT due to sequential two-photon absorption. The relative brightness of the X^{1+} to the X^0 in Fig. 1(e) indicates that the lifetime of the optically generated hole is long compared to the lifetime of the exciton. The electron-hole exchange interaction in the X^{1+} configuration will vanish since the two holes in the red QD form a singlet. Hence, the two lines in Fig. 3(b) effectively correspond to emission from an electronic singlet or triplet state formed by pure indirect electron-electron exchange. (A similar two-electron coupling, but for the ground state, was studied in Ref. [14].) Figures 3(c) and 3(d) show the DT signal at a gate bias of 106.5 mV. By using a linearly polarized resonant laser, we find that the higher energy transmission dip that corresponds to the three triplet states has an area close to 3 times that of the lower energy one that corresponds to the singlet state. The splitting between the dips is about 8.5 μeV. The electron tunneling rate corresponding to the measured splitting is found to be $t_e \approx 140$ μeV which is in excellent agreement with the previously estimated value of $t_e = 137$ μeV for CQD1.

Figure 3(d) shows the strong polarization dependence of the absorption peaks depicted in Fig. 3(c). The resonance is clearly visible with linear polarized light, but with a circular polarized laser, it is substantially suppressed. The optical selection rules do not allow for two-photon absorption leading to X^{1+} state for circularly polarized laser excitation, provided that the hole-spin lifetime is longer than the spontaneous emission time.

In conclusion, we have demonstrated coherent coupling between two stacked QDs in the regime where the widely known electron-electron exchange is suppressed enough allowing electron-hole exchange to play a prominent role. We identify the underlying mechanisms for the significant qualitative differences in the spectrum as compared to the strong interdot electron exchange case. Further, we managed to probe the opposite regime of vanishing electron-hole exchange as well by gate-tuning to a double-resonance in absorption. In addition, we expect that the optical charge sensing that we used to identify the charging states in our system will itself be a very valuable tool for applications in quantum information processing such as single spin measurement via spin-charge conversion [15,16].

This work was supported by NCCR Quantum Photonics (NCCR QP), research instrument of the Swiss National Science Foundation (SNSF). Y. Z. wishes to acknowledge funding from LGFG.

[1] P. Michler, A. Kiraz, C. Becher, W. V. Schoenfeld, P. M. Petroff, L. Zhang, E. Hu, and A. Imamoglu, Science **290**, 2282 (2000).

[2] S. Seidl, M. Kroner, P. A. Dalgarno, A. Hogele, J. M. Smith, M. Ediger, B. D. Gerardot, J. M. Garcia, P. M. Petroff, and K. Karrai *et al.*, Phys. Rev. B **72**, 195339 (2005).

[3] H. J. Krenner, M. Sabathil, E. C. Clark, A. Kress, D. Schuh, M. Bichler, G. Abstreiter, and J. J. Finley, Phys. Rev. Lett. **94**, 057402 (2005).

[4] E. A. Stinaff, M. Scheibner, A. S. Bracker, I. V. Ponomarev, V. L. Korenev, M. E. Ware, M. F. Doty, T. L. Reinecke, and D. Gammon, Science **311**, 636 (2006).

[5] M. Scheibner, M. F. Doty, I. V. Ponomarev, A. S. Bracker, E. A. Stinaff, V. L. Korenev, T. L. Reinecke, and D. Gammon, Phys. Rev. B **75**, 245318 (2007).

[6] H. J. Krenner, E. C. Clark, T. Nakaoka, M. Bichler, C. Scheurer, G. Abstreiter, and J. J. Finley, Phys. Rev. Lett. **97**, 076403 (2006).

[7] M. F. Doty, M. Scheibner, I. V. Ponomarev, E. A. Stinaff, A. S. Bracker, V. L. Korenev, T. L. Reinecke, and D. Gammon, Phys. Rev. Lett. **97**, 197202 (2006).

[8] The anticipated lateral size of the QDs is 20–30 nm, and the height is set by the partial coverage.

[9] B. Alen, F. Bickel, K. Karrai, R. J. Warburton, and P. M. Petroff, Appl. Phys. Lett. **83**, 2235 (2003).

[10] R. J. Warburton, C. Schäflein, F. B. D. Haft, A. Lorke, K. Karrai, J. M. Garcia, W. Schoenfeld, and P. M. Petroff, Nature (London) **405**, 926 (2000).

[11] M. Ediger, P. A. Dalgarno, J. M. Smith, B. D. Gerardot, R. J. Warburton, K. Karrai, and P. M. Petroff, Appl. Phys. Lett. **86**, 211909 (2005).

[12] The splitting of the red X^0 line in Fig. 2(c) would correspond to an exciton g-factor of only 0.6, which is the expected contribution from the electron. Considering the unusual energy of X^{+1} relative to X^0, we could argue that the stacked QD has different shape and different strain in and around the QD, changing the exciton g-factor ([13]). The X^{-1} line of the blue QD has an exciton g-factor of 1.93.

[13] T. Nakaoka, T. Saito, J. Tatebayashi, and Y. Arakawa, Phys. Rev. B **70**, 235337 (2004).

[14] H. E. Türeci, J. M. Taylor, and A. Imamoglu, Phys. Rev. B **75**, 235313 (2007).

[15] M. Field, C. G. Smith, M. Pepper, D. A. Ritchie, J. E. F. Frost, G. A. C. Jones, and D. G. Hasko, Phys. Rev. Lett. **70**, 1311 (1993).

[16] J. M. Elzerman, R. Hanson, L. H. W. van Beveren, B. Witkamp, L. M. K. Vandersypen, and L. P. Kouwenhoven, Nature (London) **430**, 431 (2004).